Chem Soc Rev

Structure, Function, Self-Assembly, and Applications of Bottlebrush Copolymers

Journal:	*Chemical Society Reviews*
Manuscript ID:	CS-REV-09-2014-000329.R1
Article Type:	Review Article
Date Submitted by the Author:	04-Feb-2015
Complete List of Authors:	Verduzco, Rafael; William Marsh Rice University, Chemical and Biomolecular Engineering; William Marsh Rice University, Materials Science and NanoEngineering; William Marsh Rice University, The Smalley Institute for Nanoscale Science and Technology Li, Xianyu; William Marsh Rice University, Chemical and Biomolecular Engineering Pesek, Stacy; Rice University, Chemical and Biomolecular Engineering Stein, Gila; University of Houston, Department of Chemical and Biomolecular Engineering

SCHOLARONE™
Manuscripts

Structure, Function, Self-Assembly, and Applications of Bottlebrush Copolymers

Rafael Verduzco[1,2],*, Xianyu Li[1], Stacy L. Pesek[1], and Gila E. Stein[3]

[1]William Marsh Rice University, 6100 Main Street, Department of Chemical and Biomolecular Engineering, MS-362. Houston, TX 77005.

[2]William Marsh Rice University, 6100 Main Street, Department of Materials Science and Nano Engineering, MS-325. Houston, TX 77005.

[2]Department of Chemical and Biomolecular Engineering, University of Houston, Houston TX 77204

KEYWORDS

ABSTRACT

Bottlebrush polymers are a type of branched or graft polymer with polymeric side-chains attached to a linear backbone, and the unusual architecture of bottlebrushes provides a number of unique and potentially useful properties. These include a high entanglement molecular weight, enabling rapid self-assembly of bottlebrush block copolymers into large domain structures, the self-assembly of bottlebrush block copolymer micelles in a selective solvent even at very low dilutions, and the functionalization of bottlebrush side-chains for recognition, imaging, or drug

delivery in aqueous environments. This review article focuses on recent developments in the field of bottlebrush polymers with an emphasis on applications of bottlebrush copolymers. Bottlebrush copolymers contain two (or more) different types of polymeric side-chains. Recent work has explored the diverse properties and functions of bottlebrush polymers and copolymers in solutions, films, and melts, and applications explored include photonic materials, bottlebrush films for lithographic patterning, drug delivery, and tumor detection and imaging. We provide a brief introduction to bottlebrush synthesis and physical properties and then discuss work related to: i) bottlebrush self-assembly in melts and bulk thin films, ii) bottlebrushes for photonics and lithography, iii) bottlebrushes for small molecule encapsulation and delivery in solution, and iv) bottlebrush micelles and assemblies in solution. We briefly discuss three potential areas for future research, including developing a more quantitative model of bottlebrush self-assembly in the bulk, studying the properties of bottlebrushes at interfaces, and investigating the solution assembly of bottlebrush copolymers.

Introduction

Bottlebrush polymers are a type of branched or graft polymer with polymeric side-chains attached to a linear backbone (see Fig. 1). By definition, bottlebrush polymers have one or more polymeric side-chain attached to each repeat unit of a linear polymer backbone, leading to a high side chain grafting density. This unusual architecture leads to a number novel and potentially useful properties. For example, unlike linear block copolymers, high molecular weight bottlebrush block copolymers do not entangle and can self assemble to form structures with large domain sizes, up to several hundred nanometres. Bottlebrush block copolymers form micelles in a selective solvent, but have a much lower critical micelle concentration compared with linear

diblock copolymers and surfactants, thereby enabling applications such as detection or sensing in biological media that require dilute conditions. Bottlebrush polymer side-chains can be tailored for solubility or functionalized with elements for imaging and recognition.

This review article focuses on recent developments in the field of bottlebrush polymers with an emphasis on applications of bottlebrush copolymers. Bottlebrush copolymers are made by attaching polymeric side-chains of two (or more) different types of comonomers, as in the example shown in Fig. 1D. The architectures include bottlebrush block copolymers, bottlebrush copolymers with mixed side-chains, and core-shell bottlebrush polymers with block copolymer side-chains (Fig. 6C). Applications of bottlebrush copolymers include nanocarriers for drug delivery[1], stimuli-responsive coatings[2], photonics[3], and lithographic patterning[4].

Bottlebrush polymers were first synthesized in the early 1980s[5,6], and early work was primarily focused on the development of polymer synthesis strategies. The application of controlled polymerization techniques - especially controlled radical polymerizations and ring-opening polymerizations - has enabled the preparation of bottlebrush polymers with a desired backbone and side-chain length and complex structures, including block copolymer and core-shell bottlebrushes. The field has also advanced significantly in the understanding of physical properties of bottlebrushes, and work is increasingly focused on bottlebrush assemblies in unique environments rather than the conformation of individual bottlebrushes. Interest in bottlebrush polymers, as measured by literature citations, has grown steadily over the past two decades (Fig. 2).
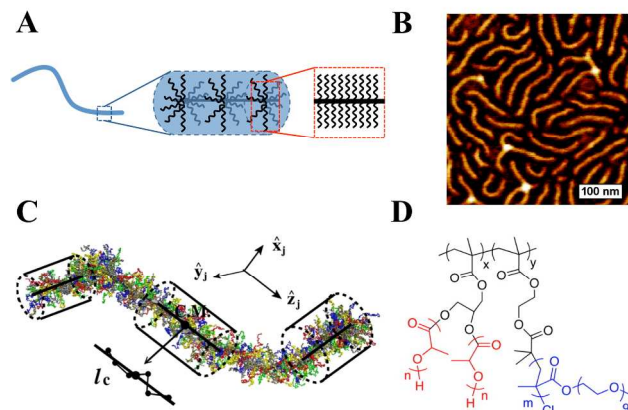
Fig. 1. Molecular structures, schematics, and simulation snapshots of bottlebrush polymers. A) Schematic of a bottlebrush polymer, adapted with permission from Pesek et al.[7] Copyright (2013) American Chemical Society. B) Atomic force microscopy (AFM) image of bottlebrush polymers on a mica substrate, reprinted with permission from Nese et al.[8] Copyright (2010) American Chemical Society. C) Simulation snapshot of a bottlebrush polymer with a backbone degree of polymerization (DP) of 387 and a side-chain DP of 48. Reprinted with permission from Hsu et al. [9], Copyright (2009) American Physical Society. D) An example of a bottlebrush block copolymer, reprinted with permission from Fenyves et al.[10] Copyright (2014) American Chemical Society.

A number of bottlebrush polymer Review and Perspective articles have appeared over the last decade. A Viewpoint article by Rzayev highlights the potential of bottlebrushes as building blocks for complex and functional materials[11]. Sheiko and Matyjaszewski et al. have provided a number of very informative reviews, both on bottlebrush synthesis and physical properties[12–14]. A tutorial review by Hu and Huang et al. discusses advances in the synthesis of graft and bottlebrush polymers[15]. A review article by Chen discusses work related to materials with

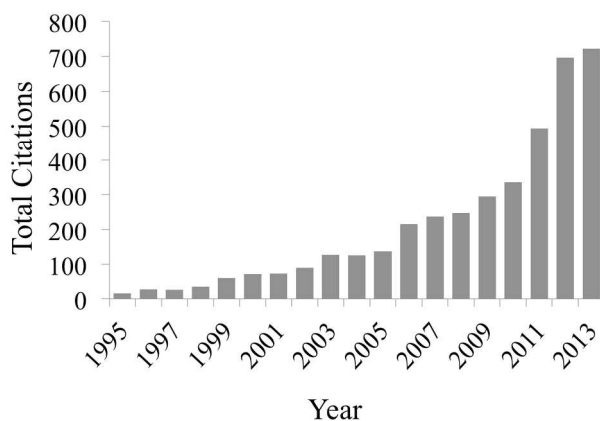densely tethered polymers, including bottlebrush polymers, polymer-coated nanoparticles, and other brushy materials[16].

Fig. 2. Total number of literature citations to publications with the words 'bottlebrush' or 'molecular brush' in the title, from Web of Science.

In this review, we will first present an overview of popular synthetic strategies, including recent advances that have made bottlebrush polymers and copolymers more synthetically accessible. Second, we will discuss the unique physical properties of individual bottlebrush polymers, both in solution and in the melt. Third, we will look at the properties and self-assembly of bottlebrush copolymers, including applications of bottlebrush copolymers in melt or bulk forms and in thin films. Finally, we will focus on bottlebrush polymers in solution, including core-shell bottlebrush polymers and bottlebrush assemblies in solution.

Synthesis of Bottlebrush Polymers

Here we provide a general overview of bottlebrush synthesis; more detailed information can be found in review articles by Matyjaszewski and Sheiko et al.[14] and by Hu and Huang et

al.[15] The synthesis of bottlebrush polymers is achieved with grafting-through, grafting-from, and grafting-to approaches (see Fig. 3). Matyjaszewski et al. first reported the grafting-from synthesis of bottlebrush polymers using a controlled radical polymerization technique[17]. In this approach, the bottlebrush backbone is synthesized first, and the side-chains are subsequently "grafted-from" the bottlebrush backbone. An advantage of the grafting-from approach is that bottlebrushes with very long backbones can be prepared. The grafting density can also be controlled by co-polymerizing two monomers during backbone synthesis[18]. Also, block copolymer side-chains can be incorporated in a straightforward way through sequential polymerization reactions, resulting in core-shell type bottlebrushes[19]. A drawback of the synthesis is that protection and deprotection of functional groups is often required, increasing synthetic complexity. The preparation of mixed or bottlebrush block copolymers is possible using grafting-from, but three or more orthogonal polymerization chemistries (or protection/deprotection steps) may be required[20].

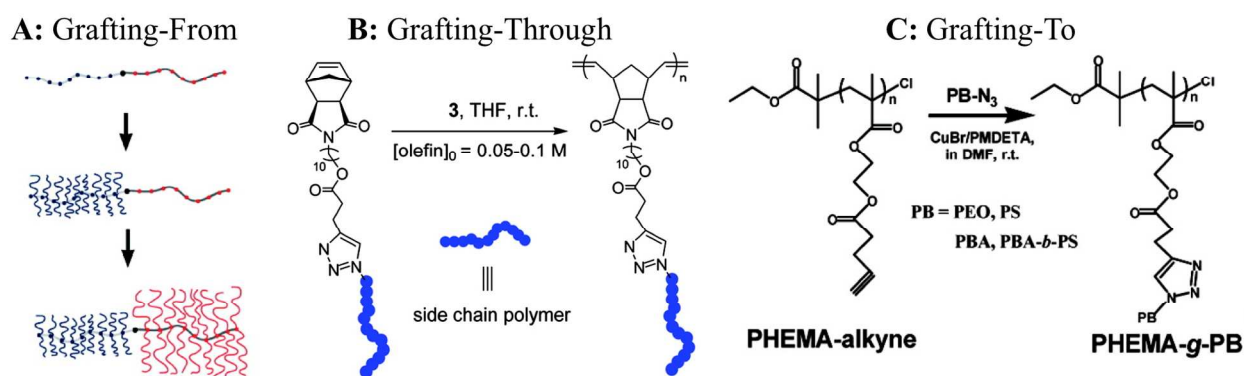**A: Grafting-From** **B: Grafting-Through** **C: Grafting-To**

Fig. 3. Examples of grafting-from, grafting-through, and grafting-to bottlebrush polymer synthesis approaches. A) Schematic of a grafting-from synthesis, adapted with permission from Bolton et al.[21] Copyright (2012) American Chemical Society. B) Schematic of a grafting-through synthesis, reprinted with permission from Xia et al.[22] Copyright (2009) American Chemical

Society. C) Example of a grafting-to synthesis approach and corresponding GCP traces, reprinted with permission from Gao et al.[23] Copyright (2007) American Chemical Society.

The grafting-through synthesis approach starts with the preparation of reactive polymeric side-chains also known as macromonomers. The macromonomers are then polymerized to form a bottlebrush polymer, and different backbone lengths can be obtained by varying the relative concentration of macromonomer to catalyst or initiator during polymerization. Solution viscosities can be very high at moderate macromonomer concentrations due to the high molecular weight of the macromonomers, and therefore highly active catalysts are needed to achieve significant conversion and control over molecular weight. Early studies implemented free radical polymerization, but macromonomer conversion was low $(30 - 80\%)$[6,24–26]. A series of bottlebrush polymers were produced using this technique and studied in solution[27–31]. Ring opening metathesis polymerization (ROMP) of norbornenyl macromonomers has been shown to be an effective grafting-through synthesis strategy, such as the example shown in Fig. 3B[22]. Bowden et al. first demonstrated the grafting-through synthesis of bottlebrush polymers by ROMP[32]. Subsequently, in 2008, Xia and Grubbs et al. reported the use of a highly-active ruthenium catalyst for achieving improved control over bottlebrush molecular weight and molecular weight dispersity[22,33]. The reactivity of norbornenyl macromonomers in ROMP is sufficient for achieving high macromonomer conversions for a range of concentrations and macromonomer molecular weights, enabling the preparation of bottlebrush polymers with systematically varying backbone and side-chain lengths.

An advantage of the ROMP grafting-through method is its simplicity. Bottlebrush polymers can be prepared in two steps using controlled polymerization for macromonomer

synthesis followed by ROMP for bottlebrush synthesis, and no protection/deprotection chemistry is required. Furthermore, mixed (Fig. 1c) and block (Fig. 1d) bottlebrush polymers can be prepared through sequential or mixed ROMP polymerization reactions of different macromonomers, as reported in several examples discussed below. A drawback of the synthetic method is that unreacted macromonomer can be hard to remove from the final product. Also, achieving large backbone DPs can be difficult. As shown in Table 1 below, typical backbone DPs for bottlebrushes made by grafting through are in the range of 100 – 400, while grafting-from strategies have produced backbone DPs greater than 1000.

The grafting-to synthesis approach involves the preparation of the bottlebrush backbone and side-chains separately, followed by a "grafting-to" coupling reaction that attaches the side-chains to the backbone. This approach faces some of the same challenges of the grafting-through approach, such as low reactivity of polymeric reagents, with the additional complication that the coupling reaction must overcome steric interactions between side-chains to achieve high grafting densities. As a result, grafting-to generally produces bottlebrush polymers with grafting densities of 60 % or lower[23,34–36,23,37], although some examples of grafting efficiencies greater than 95 % have been reported[38]. Khan et al. reported an efficient grafting-to procedure relying on thiol-epoxy coupling and giving grafting efficiencies in excess of 88 %[39,40].

Each synthetic approach has advantages and disadvantages. Table 1 compares representative examples prepared using each synthetic approach. The grafting-to approach has not been widely used because it typically produces bottlebrushes with low (< 60 %) grafting densities, but it provides a modular approach to bottlebrush synthesis and the opportunity to independently characterize the bottlebrush backbone and side-chains. The grafting-from strategy is capable of producing bottlebrush polymers with extremely long backbones and with block

copolymer side-chains, and the side-chain grafting density can be more easily controlled. The grafting-through strategy guarantees full grafting density of the backbone, and bottlebrush polymers with different side-chains can be easily prepared by carrying out sequential or one-pot polymerization reactions with different polymeric macromonomers. The side-chain and/or backbone DPs are generally lower when using the grafting-through approach due to low conversions at lower catalyst concentrations and when reacting high molecular weight macromonomer.

The advantages and disadvantages of each synthetic approach are relevant for the development of bottlebrush polymers for specific applications. The grafting-from approach is more scalable and versatile in terms of the different types and quantities of bottlebrushes that have been produced[14]. This approach would be optimal for applications involving bulk materials or bottlebrush coatings. The grafting-to approach produces bottlebrushes with lower grafting densities, which may be of interest for coatings and additives. The grafting-through approach provides a straightforward approach to bottlebrush block copolymers with uniform side-chain grafting densities, which is beneficial for fundamental studies of structure and function, but has also been used to synthesize bottlebrushes for imaging and detection[41,42]. The grafting-through approach has been reported for the large-scale synthesis of polyolefin bottlebrush polymers[43].

In addition to the examples discussed above, a number of other polymer synthesis strategies have been reported. Bottlebrush polymers can be synthesized by Suzuki polycondensation[44,45], chain-growth polycondensation[46], cyclopolymerization[47], sequential ROMP polymerizations[48], nonliving transition metal catalysis[49], combination of grafting-to and grafting-from[35,50], and multiple controlled radical polymerization reactions[51]. Novel bottlebrush architectures include dumbbell shaped bottlebrushes[52], block miktobrushes[53],

polypseudorotaxanes[54], bottlebrush polymers with dendritic side-chain endgroups[55], and

bottlebrush polymers with a redox-responsive backbone[56].

Table 1. Selected examples of bottlebrush polymers prepared by the grafting-from,

grafting-through, and grafting-to synthetic approaches.

Synthesis Strategy	Backbone		Side-Chain		Grafting Density	Ref.
	Type[a]	*DP*	*Type*[a]	*DP*		
Grafting-From	MA	2150	P*n*BA	12 – 140	100%	57
	MA	275	PDMAEMA	73	100%	58
	MA	380	PLA, PS	15 – 45	100%	59
	MA	341	P*n*BA	33	33%	18
	MA	3600	P*n*BA	140	100%	60
	NB	130	PMMA	72	65%	61
	MA	320-630	PLA, PS	18 – 35	100%	62
	MA	428	PLA, PS	26 – 45	100%	21
	NB	525	PLA	100 – 347	100%	32
Grafting-Through	ONBA	10	PEO	45	100%	63
	NB	50 – 1020	PLA	30 – 68	100%	32
	NB	300	P*t*BA	130	100%	64
	NBA	50 – 400	PMA, PS, P*t*BA	17 – 66	100%	22
	NBA	100 – 400	PS, P*t*BA, PS, PLA	17 – 66	100%	33
	NB	95	PS-*b*-PMA-*b*-PAA	132	100%	65
	NB	25-170	P3HT	12	100%	66
	NBA	237 – 653	PHIC, PBI	30 – 50	100%	3
Grafting-To	MA	210	PEO, PS, P*n*BA, P*n*BA-*b*-PS	7 – 46	20 – 62%	23
	PBLG	360	PEG	8	20 – 36%	67
	MA	180 – 323	PEG	1 – 42	88 – 97 %	39
	PLL	150 – 2200	PEG	22 – 113	48%	68
	PLLGA	9	PEG	11 – 114	96 – 99%	38
	PCEVE	845	PS	60	77%	35

[a]abbreviations for polymer backbones and side-chains: MA (methacrylate); NB (norbornene); ONBA (oxanorbornene anhydride); NBA (norbornene anhydride); P*n*BA poly(*n*-butyl acrylate); PDMAEMA (poly(2-(dimethylamino)ethyl methacrylate); PMMA (poly(methyl methacrylate)); PLA (poly(lactic acid)); PS (polystyrene); P*t*BA (poly(t-butyl acrylate)); PAA (poly(acrylate acid)); P3HT(poly(3-hexylthiphone)); PHIC (poly(hexyl isocyanate)); PBI (poly(4-phenyl butyl isocyanate)); PMA (polymethacrylate)); PBLG (poly(γ-benzyl-l-glutamate)); PEG (poly(ethylene glycol)); PLL (poly (L-lysine)); PLLGA (γ-poly(-propargy-L-glutamate)); PCEVE (poly(chloroethyl vinyl ether))

Bottlebrushes with Homopolymer Side-Chains

Understanding the unique structures of bottlebrushes at surfaces, in solution, and in melts is important for assessing different potential applications. The discussion in this section is restricted to the simple case where all bottlebrush side-chains have the same composition, which serves to briefly introduce the backbone and side-chain conformations. The section that follows is focused on complex bottlebrush compositions, where the side-chains are comprised of at least two monomeric units.

Experimental and theoretical studies demonstrate that the bottlebrush polymer backbone is partially or fully extended due to steric interactions between side chains. This is true for bottlebrush polymers adsorbed to a surface or in good solvents that swell the side-chains and backbone. Sheiko et al. imaged individual bottlebrushes adsorbed at a surface with scanning force microscopy (SFM), and these data clearly demonstrate a stretched backbone conformation see Fig. 4A) [18,69–74]. Rathgeber et al. carried out neutron, X-ray, and computer simulation studies to analyze the conformation of bottlebrushes in solution[75–77]. They found that scattering spectra for bottlebrush polymers were accurately represented by worm-like chain models (see Fig. 4B). Verduzco et al. carried out small-angle neutron scattering measurements (SANS) that demonstrated backbone stretching through a systematic change in bottlebrush aspect-ratio (from spherical to cylindrical) with increasing backbone degree of polymerization (DP) (see Fig. 4C)[7]. This conformational transition was also reflected in rheological studies of bottlebrush melts for different backbone DPs[78].
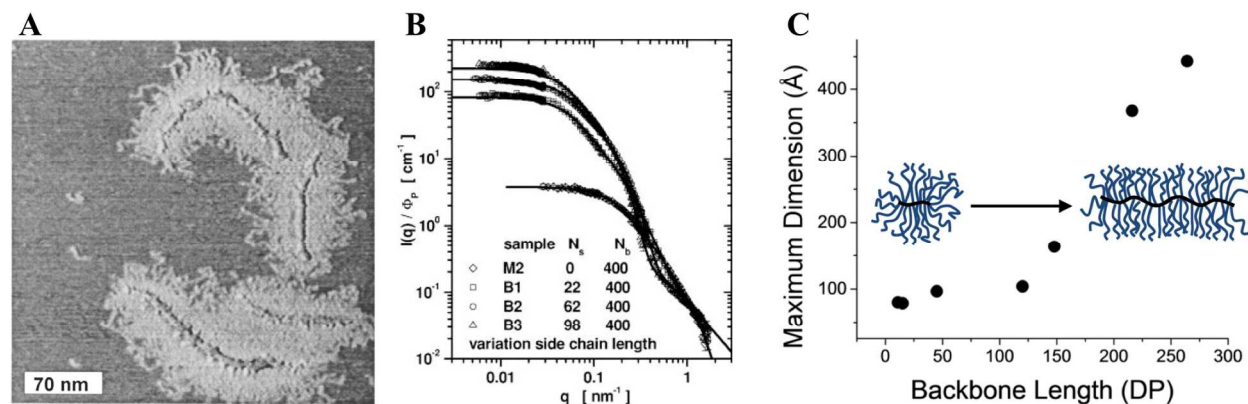
Fig. 4. Selected examples of experimental studies of homopolymer bottlebrush polymers on a surface and in solution. A) Scanning force microscopy (SFM) image of bottlebrush polymers adsorbed to a surface, reprinted with permission from Sheiko et al.[69] Copyright (2001) American Chemical Society, B) Small-angle neutron scattering (SANS) and light-scattering data from bottlebrush polymers in a good solvent along with curves from a worm-like chain model, reprinted with permission from Rathgeber et al.[77] Copyright (2005) AIP Publishing, and C) molecular parameters and schematic of the changing conformation of bottlebrush polymers with backbone length from SANS analysis, reprinted with permission from Pesek et al.[7], Copyright (2013) American Chemical Society.

The bottlebrush side-chain conformations will vary in different states (adsorbed, solvent, melt), but when their grafting density is high, the side-chains are more extended than free linear polymers of the same DP (denoted by N). To underline this point, we review the bottlebrush "size" (width or radius) as a function of N, and we omit pre-factors that depend on solvent quality, grafting density, backbone structure, and Kuhn length. The side-chain conformations of bottlebrushes adsorbed at a solid-air interface (2D) have been studied with experiments (SFM) and theory, and the outcomes demonstrate that side-chains stretch along one direction with an

end-to-end distance proportional to N.[22,79] For comparison, free polymers adsorbed at a planar surface exhibit an isotropic 2D conformation with an end-to-end distance that scales with $N^{1/2}$. The side-chain conformations of bottlebrushes in a bulk melt or solution (3D) cannot be directly imaged with SFM, but theoretical models based on blob-type depictions of brushes yield simple scaling laws. In a good solvent, the bottlebrush radius is predicted[79–83] to scale with $N^{3/4}$ while the radius of free linear chains scales with $N^{3/5}$. The bottlebrush and linear power laws N^{δ} are consistent with 2D ($\delta=3/4$) and 3D ($\delta=3/5$) self-avoiding walks, but in the case of a bottlebrush, it is important to note that side-chain conformations within the 2D plane are highly anisotropic.[82] In a theta solvent, the bottlebrush radius is predicted to scale with $N^{2/3}$ or $N^{3/4}$, depending on the model assumptions,[80,84] while the radius of free linear chains scales with $N^{1/2}$ (ideal chain). The bottlebrush is even stretched in a poor solvent: the bottlebrush radius is predicted to scale as $N^{1/2}$,[84] while the radius of free linear chains scales as $N^{1/3}$. The predicted scaling behaviour of bottlebrushes in a melt is $N^{1/2}$,[84] and while free linear chains exhibit the same scaling, these systems differ in their anisotropy (quasi-2D vs. 3D). These simple scaling laws can guide materials design and aid the interpretation of small angle scattering measurements. However, simulations have noted that theoretical predictions may fail for side-chain lengths on the order of $N \sim 10 - 100$,[82,85,86] which is typical of many experiments.

The extended backbone and side-chain conformations are responsible for many unique properties. For example, bottlebrush polymer melts exhibit unusual rheological behaviour due to their very high entanglement molecular weights.[78,87] Furthermore, the elongated conformation of bottlebrush polymers may be beneficial for nanocarrier applications, since nanoparticle shape is important for retention times and the bodies' immune response[88]. A potential drawback of

backbone stretching is backbone cleavage when a bottlebrush adsorbs onto a surface or is subjected to shear[84,89,90].

While side-chains are stretched compared with free linear chains, they exhibit significant conformational flexibility. This is reflected in studies of the self-assembly of random bottlebrush polymers[33] and stimuli-responsive properties of bottlebrush polymers[2] with mixed side chains. The high side-chain grafting density also leads to potentially useful phase behaviour in blends. As demonstrated by Sheiko et al., bottlebrush polymers undergo autophobic dewetting when blended with a linear polymers of the same composition as the bottlebrush polymers and of a sufficiently high molecular weight (see Fig. 5A) [74]. Stein and Verduzco et al. demonstrated that this could be used as an effective method to drive bottlebrushes to interfaces (see Fig. 5B)[91], which might be desirable for applications such as antifouling.
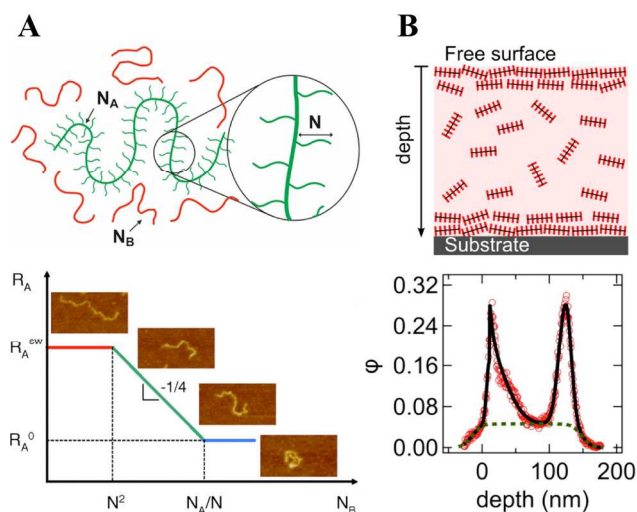

Fig. 5. Phase behaviour and conformational changes in blends of bottlebrush polymers with linear polymers. A) Schematic for mixing of linear and bottlebrush polymers and SFM studies of conformational changes of bottlebrush polymers with changing linear and bottlebrush polymer side-chain length. Reprinted with permission from Sheiko et al.[74] Copyright (2007) by the American Physical Society. B) Schematic for the segregation of bottlebrush polymer to film

interfaces when blended with linear polymers and secondary ion mass spectroscopy data showing bottlebrush enrichment at film interfaces. Reprinted with permission from Mitra et al. [91] Copyright (2014) the American Chemical Society.

Xia et al. studied the dynamics of the side-chains and backbone using electron paramagnetic resonance (EPR).[92] They placed nitroxide radical probes at different locations along a PLA bottlebrush – either in the middle of the backbone, at the backbone ends, or on the side-chain ends. Rotational correlation times were roughly two orders of magnitude shorter for side-chain ends compared with the backbone, indicating much faster dynamics of side-chain ends. Through reactive quenching experiments, they also showed that the side-chain ends were accessible to both small molecular and polymeric reagents, while the backbone nitroxide probes reacted with small molecule quenchers but only slowly to polymeric quenchers.   Zhang et al. used simulations to study conformational relaxations of PLA bottlebrushes. They found that the length of the side-chains could influence conformational relaxation times of the backbone, with longer side-chains resulting in slower conformational dynamics. This was attributed both to side-chain crowding and solubility differences between the bottlebrush side-chains and backbone[93].

The unique architecture of bottlebrush polymers can be used to generate new self-assembled phases. Linear diblock and triblock copolymers self-assemble into phases driven a balance of enthalpic and entropic interactions. The architecture of bottlebrush polymers (extended backbone, densely grafted side-chains) results in qualitatively new self-assembly behaviour of bottlebrush copolymers, discussed in examples below.

Bottlebrush Copolymers: Mixed, Random, Block Copolymer, and Core-Shell

Bottlebrush copolymers have side-chains comprised of two or more monomeric units. Similar to graft copolymers[94], there are a number of different ways to structure bottlebrush copolymers: block copolymer and mixed side-chain bottlebrushes are prepared by attaching two or more different types of side-chains to the bottlebrush backbone. In the case of bottlebrush block copolymers, the side-chains are arranged into distinct "blocks" (see Fig. 6A), similar to the traditional linear block copolymers. Bottlebrush block copolymers self-assemble to form large domains and exhibit very high order-to-disorder transition temperatures due to the extended backbone and sterically-interacting side chains, as discussed in several examples below. Mixed side-chain bottlebrush polymers (Fig. 6B) have two or more chemically distinct side-chains attached to the backbone. Subsets of mixed side-chain bottlebrushes include random or alternating side-chain bottlebrush copolymers. A third type of bottlebrush copolymer is prepared by attaching linear block copolymers as side-chains, forming core-shell type bottlebrushes (Fig. 6C). In addition to these general classes of bottlebrush copolymers, combinations of the different types can be prepared. For example, bottlebrushes can be both block copolymer and core-shell[95]. Also, three of more different types of side-chains can be incorporated[20,96].

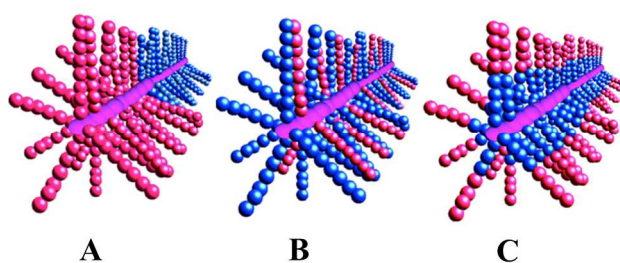**A**   **B**   **C**

Fig. 6. Structures of bottlebrush copolymers: A) bottlebrush block copolymers; B) random, mixed bottlebrush copolymers; C) and core-shell bottlebrush copolymers. Adapted with permission from Lanson et al.[36] Copyright (2009) American Chemical Society.

Block copolymer, mixed, and core-shell bottlebrush copolymers provide new opportunities for developing nanostructured materials through self-assembly, either in solution, in thin films, and in the bulk. In the following three sections, we discuss properties, structure, and function of each type of bottlebrush copolymer in different environments. We first discuss work investigating bottlebrush copolymers in the bulk and in thin films. Second, we discuss the structure and applications of non-associating bottlebrush copolymers in solution. Finally, we discuss the development and properties of bottlebrush copolymers that self-assemble in solution.

Bulk and Thin Film Self-Assembly of Bottlebrush Block Copolymers

Bottlebrush block copolymers readily self-assemble to form much larger domains than those typically observed in linear block copolymers. Bowden et al. first demonstrated this by synthesizing a series of high molecular weight bottlebrush block copolymers with polystyrene (PS) and poly(lactic acid) (PLA) arms[97]. These bottlebrush block copolymers formed large 100 – 200 nm cylindrical domains (see Fig. **7**A). Subsequently, the same group found similar self-assembly behaviour in a series of brush-linear diblock copolymers[98,99]. Scanning electron microscopy (SEM) and UV-Vis absorbance analysis revealed the formation of large block copolymer domains ranging in size from 100 – 300 nm with morphologies in the lamellar, cylindrical, or spherical phase depending on the relative block lengths. Bowden and co-workers later demonstrated the synthesis and self-assembly of high molecular weight di-, tri-, and tetrablock copolymers[96] and the synthesis of bottlebrush block copolymers with different side-chains and backbones[100]. This work established the concept of bottlebrush block copolymers assembling to form large domains and also demonstrated that asymmetric bottlebrush block copolymers could form similar phases (cylindrical, lamellar, spherical) as observed for linear

block copolymers. They also measured changes in domain sizes and phases with changing side-chain and backbone lengths, and found that the phase morphology could be tuned by changing the side-chain length while the domain size depended strongly on backbone length.
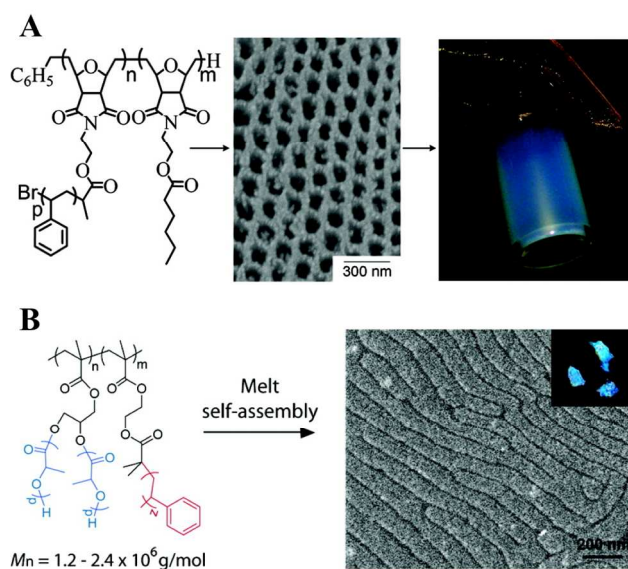

Fig. 7. Self-assembly of bottlebrush block copolymers into large domains in the bulk. A) Cylindrical phase in bottlebrush comb-linear copolymers, reprinted with permission from Runge et al.[98] Copyright (2007) American Chemical Society. B) Lamellar domains in bottlebrush block copolymers. Reprinted with permission from Rzayev et al. Copyright (2009) the American Chemical Society[62].

Rzayev et al. prepared a series of bottlebrush block copolymers with PS and PLA arms. In contrast to the initial report on similar bottlebrush copolymers from Bowden et al[97] where the PS and PLA side chains were larger than 10 kg/mol, the bottlebrush copolymers reported by Rzayev contained shorter side chains, roughly 1 − 5 kg/mol, but had a higher backbone grafting density. The bottlebrush copolymers self-assembled to form lamellar domains ranging in size from 70 − 150 nm, as evidenced by small-angle X-ray scattering (SAXS), SEM, and visual

analysis (see Fig. 7B.). Lamellar ordering was found in all samples except for those short or asymmetric side-chain lengths. Rzayev also reported a linear dependence of domain size with molecular weight, which contrasts with the $\sim N^{2/3}$ dependence observed in linear block copolymers in the strong segregation regime[101,102] and indicates that the backbone is locally aligned along a 1-D axis. Rzayev further demonstrated that asymmetric bottlebrush block copolymers, which contain different side-chain lengths but similar backbone lengths of each block, can self-assemble into cylindrical morphologies. This was shown to give nanoporous materials with large (~ 50 nm) cylindrical channels.[59] Recently, Rzayev et al. reported the synthesis of triblock bottlebrush copolymers with PS, PLA, and poly(methyl methacrylate) (PMMA) blocks. The triblock bottlebrush copolymers assembled into a lamellar phase with domain spacing comparable to PS-PLA bottlebrushes of a similar backbone length. Surprisingly, the PS and PMMA bottlebrush blocks appeared to be mixed (but segregated from the PLA domains) based on differential scanning calorimetry (DSC) analysis[20].

In 2009, Xia and Grubbs et al. reported block copolymer and random bottlebrush polymers prepared by grafting-through ROMP (see Fig. 8A) [22,33]. The synthetic strategy was similar to that reported by Bowden et al.[32], but the use of third-generation Grubbs catalyst enabled bottlebrush polymers with low molecular weight dispersities (< 1.05), backbone DPs up to 400, and side-chain MWs up to 7000 g/mol. Symmetric bottlebrush block copolymers with similar PLA and poly(*n*-butyl acrylate) (P*n*BA) side-chain and backbone lengths formed exclusively lamellar domains with periodicities larger than 100 nm. Asymmetric bottlebrushes with longer P*n*BA blocks (backbone DP ratios of 20:180 and 40:160 for PLA:P*n*BA blocks) formed non-lamellar phases with smaller characteristic periodicities of 40 – 60 nm. Xia and Grubbs et al. also found that bottlebrush block copolymers did not exhibit a measureable order-

to-disorder transition temperature (T_{ODT}). Thus, the extended backbone prevented coiling and the formation of a disordered block copolymer phase[33].

Russell et al. studied the structure and self-assembly kinetics of symmetric bottlebrush block copolymers through experiments and simulations[103,104]. PS-PLA bottlebrushes with matched side-chain and backbone block lengths exhibited lamellar ordering in the bulk. The lamellar periodicity L increased with backbone length N, following the power-law scaling of $L \sim N^{0.90}$. Monte-Carlo simulations predicted a similar scaling dependence for bead-spring bottlebrush block copolymers with backbone DPs of $6 - 30$ and side-chain DPs of $3 - 12$. The simulations also predicted localization of bottlebrush chain ends at the centre of lamellae rather than at the PS-PLA interface. In the same study, they analysed the kinetics for self-assembly. *In-situ* SAXS measurements showed that bottlebrush polymers formed ordered lamellar phases with multiple reflections in as fast as 1 minute for a 118 kg/mol bottlebrush block copolymer thermally annealed at 130 ℃. A larger 529 kg/mol sample took up to 1 h to self-assemble, while a comparable linear diblock of roughly 50 kg/mol did not form a fully developed lamellar phase after 24 h of thermal annealing[104].

Russell et al. extended their study of symmetric PS and PLA bottlebrushes to self-assembly in thin films. They demonstrated that in-plane lamellae (oriented perpendicular to the substrate) could be achieved on untreated substrates through solvent annealing (see Fig. 8B), in contrast to linear block copolymers where surface treatment is oftentimes required due to differential surface energies of the polymer blocks. The domain size was found to depend linearly on backbone size, and the authors found a terraced film surface indicating that bottlebrush polymers formed a monolayer on the film surface by laying flat[103]. Similar terraced films were observed in films prepared by Grubbs et al.[33]
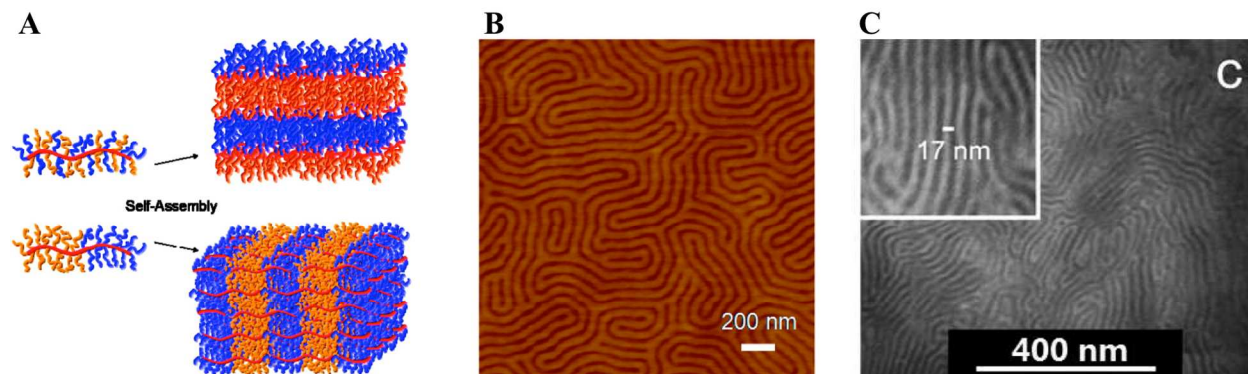
Fig. 8. Self-assembly of block and random bottlebrush copolymers through microphase segregation. A) Schematic for the self-assembly of random bottlebrushes (top) and bottlebrush block polymers (bottom). Reprinted with permission from Xia et al. [33] Copyright (2009) American Chemical Society. B) SFM height image of asymmetric bottlebrush block copolymer on an unmodified Si substrate. Reprinted with permission from the Hong et al.[103] Copyright (2013) American Chemical Society. C) TEM micrograph of a self-assembled random bottlebrush copolymer. Reprinted with permission from Hou et al.[34], Copyright (2013) American Chemical Society.

Lin et al. studied self-assembly and hierarchical ordering in bottlebrush block copolymer films deposited by evaporative assembly[105,106]. A bottlebrush solution was placed in a wedge-on-flat geometry using a wedge-shaped lens on top of a Si substrate, so the bottlebrushes were deposited in an elongated "stripe" with microscale width. Within these "stripes", the authors observed the formation of cylindrical domains through self-assembly. The cylinders transitioned from vertically-oriented to lying flat on the substrate with THF solvent annealing.

Random or mixed side-chain bottlebrush polymers can also self-assemble to form nanostructured domains, as shown schematically in Fig. 8A. Xia and Grubbs et al. synthesized a series of PLA and P*n*BA random side-chain bottlebrushes with a 1:1 ratio of side-chains and

varying in overall backbone DP. All samples prepared were self-assembled in the melt to form 14.3 nm lamellar domains, independent of backbone DP. These random bottlebrush copolymers also exhibited a T_{ODT} dependent on the side-chain length and independent of backbone length[33]. Deffieux et al. prepared random side-chain bottlebrushes with PS and poly(isoprene) (PI) side-chains which formed lamellar phases with domain sizes of 20 – 30 nm, except for one bottlebrush copolymer with a low PI content that formed a disordered phase[36]. Hu and Liu et al. reported the synthesis of random side-chain bottlebrush polymers containing P*n*BA and poly(2-cinnamoyloxyethyl methacrylate) (PCEMA) side-chains[34]. Despite low side-chain grafting densities of 20 %, random side-chain bottlebrushes self-assembled to form lamellar and cylindrical morphologies as revealed by transmission electron microscopy. The domain sizes were roughly 10 nm for P*n*BA and PCEMA lamellar domains and 6 nm for P*n*BA cylinders in a PCEMA matrix (see Fig. 8C).

Kasi et al. investigated a series of block and random bottlebrush copolymers with liquid crystal (LC) side groups as a potential route to hierarchical assembly and nanostructured materials that could be aligned by magnetic field[107–109]. Two types of LC side-groups were explored: either cholesteryl liquid crystal mesogens that display cholesteric and smectic LC phases, or a cyanobiphenyl mesogen that exhibits a smectic LC phase. Bottlebrush copolymers that incorporated the LC side-groups and either a PEG or PLA side-chain exhibited hierarchical ordering: polymer crystallization at the smallest length scales, smectic layers at 3 – 7 nm, microphase segregation at roughly 50 nm length scales, and in some cases cholesteric helices at 150 – 200 nm length scales. The materials studied contained relatively short PEG or PLA bottlebrush blocks, but microphase segregation was observed both for block and random bottlebrush copolymers. The presence of LC order enables magnetic field alignment of bulk

bottlebrush materials, and the authors demonstrated alignment of a block bottlebrush copolymer that contained LC and PLA side-chains using a magnetic field. The PLA domains were subsequently removed in acid to produce a nanoporous material[109].

These studies have established the basic self-assembly properties of bottlebrush copolymers in films and in the melt. Bottlebrush block copolymers self-assemble through microphase segregation to form large domain sizes (up to several hundred nm) dependent primarily on the backbone length. Bottlebrush block copolymers exhibit ordered phases stable to very high temperatures, due to an extended backbone which keeps bottlebrush polymer blocks segregated. A number of studies have found a linear dependence on domain size with backbone DP for symmetric bottlebrush block copolymers, and asymmetric bottlebrushes can form cylindrical or spherical phases. Random side-chain bottlebrushes self-assemble to form lamellae with smaller sizes, $10 - 20$ nm, on length scales comparable to the R_g of the side-chains. In the section that follows, we discuss examples of bottlebrush block copolymers used for thin film patterning, lithography, and photonic applications.

Bulk and Thin Film Applications of Bottlebrush Copolymers

Bottlebrush block copolymers self-assemble in the bulk and thin films producing larger domain sizes with more rapid self-assembly kinetics compared with linear block copolymers of similar molecular weights. This provides opportunities for novel applications of bottlebrush polymers for photonic crystals and lithographic patterning.

Photonic crystals are materials with a periodic variation in the dielectric constant[110]. Block copolymers can form 1-D photonic crystals, and to reflect light at visible or IR-wavelengths the domain spacing should be roughly $\lambda/4n_i$, where λ is the wavelength of light and

n_i the refractive index of each block[111]. For a polymer refractive index of 1.5, the domain spacing should be roughly 100 nm, which is typical for a wide range of bottlebrush block copolymers studied. Indeed, a number of researchers have noted the selective reflection of blue or green light in bottlebrush block copolymer films and melts[33,62,98] (see examples in Fig. 7). Grubbs et al. studied the photonic properties of a series of PS/PLA bottlebrush block copolymer to understand the role of molecular weight and processing conditions on domain size[112]. A series of symmetric (same side-chain M_W and backbone DP for each block) PS/PLA bottlebrush block copolymers were synthesized, and their optical properties were analyzed after drop casting or thermal annealing under pressure (in a polymer melt press). Drop cast samples exhibited different reflection bands when cast from different solvents, but were poorly ordered compared with thermally annealed samples. Thermally annealed samples exhibited a narrower reflection band that varied linearly (from 200 – 600 nm) with total molecular weight, expected based on prior self-assembly studies discussed above. Reflection bands at IR wavelengths were also achieved by melt pressing bottlebrush samples. For comparison with linear diblock copolymers, such long-wavelength reflection bands have only been observed in solvent-swollen block copolymer gels[113].
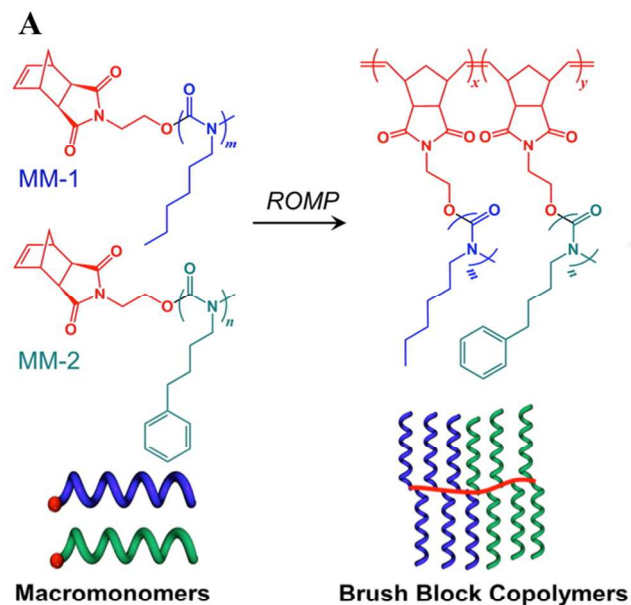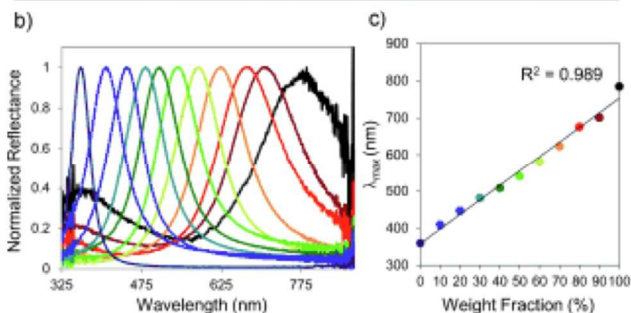
Fig. 9. Photonic crystals based on bottlebrush block copolymers. A) Structure and schematic of poly(isocyanate) based bottlebrush polymers. Reprinted with permission from Miyake et al.[114] Copyright (2012) American Chemical Society. B) Example of photonic crystals formed through blending two different brush block copolymers, including reflectance spectra and peak reflectance. Reprinted with permission from Miyake et al.[3] Copyright (2012) Wiley.

To improve the assembly of bottlebrush block copolymers under solvent casting and annealing, Grubbs et al. explored a series of bottlebrush block copolymers with poly(isocyanate) side-chains (see Fig. 9). Poly(isocyanate) side-chains were chosen due to their rigidity and expected rapid assembly compared with more flexible side-chains. Symmetric, block poly(isocyanate) bottlebrush copolymers were demonstrated to form 1-D photonic crystals by solvent casting, with tuning of the peak reflectance over a wide range, from 200 – 1200 nm, by varying the bottlebrush molecular weight. Interestingly, the reflection band broadened with increasing domain size due to a loss of long-range ordering with increasing bottlebrush molecular weight[114]. Grubbs et al. then demonstrated a simple approach to obtain tuneable 1-D photonic crystals through blending. Two symmetric bottlebrush block copolymers were synthesized, one small (1.5×10^6 g/mol, backbone DP = 236) and one large (4.2×10^6 g/mol, backbone DP = 653). The smaller bottlebrush block copolymer exhibited a selective reflection band at roughly 360 nm, while the larger had a reflective band at 785 nm. The selective reflection band could be tuned between these two limits by blending the larger and smaller bottlebrushes. The peak reflection varied linearly with composition, indicating a linear dependence of domain size on composition[3]. These examples demonstrate the potential utility of bottlebrush block copolymers as rapidly assembling photonic crystals. Grubbs et al. also demonstrated the assembly of dendronized polymers containing short and bulky side-groups. These assembled rapidly on solvent casting and exhibited a tuneable selective reflection band over a broad range of wavelengths[115].

Verduzco et al. studied the properties of mixed side-chain bottlebrushes with PEG and PS side-chains. Bottlebrushes were deposited on a surface by spin casting, and surface properties were analysed by microscopy, contact angle measurements, and X-ray photoelectron

spectroscopy (XPS). The authors found that the water contact angle and composition at the film surface could be changed by exposure to selective solvents, and the change in contact angle and composition was more significant for bottlebrushes with longer side-chains. Similar behaviour occurs in polymer brush surface coatings[116]. The work demonstrates the potential of bottlebrush polymers as solution-processible brush coatings for preparing functional surfaces[2].

Wooley et al. investigated the use of bottlebrush block copolymers as chemically amplified resists[117,4,118]. Their approach takes advantage of the self-assembly of bottlebrush block copolymers to reduce randomness in molecular orientation in spun-cast thin films. Bottlebrush block copolymers with a short, fluorinated side-chain segment poly(tetrafluoro-*p*-hydroxystyrene) (PTF*p*HS) and a longer, crosslinkable poly(*p*-hydroxystyrene-*co*-*N*-phenylmaleimide) [P(*p*HS-*co*-PhMI)] segment oriented vertically due to the lower surface energy of the fluorinated PTFpHS block. This preferential vertical orientation improved under solvent annealing with acetone, as determined by X-ray photoelectron spectroscopy (XPS) and secondary ion mass spectroscopy (SIMS). In comparison to both a linear diblock copolymer control and a bottlebrush control lacking the PTF*p*HS segment, the bottlebrush block copolymers exhibited patterns with narrower line widths, as small as 10 nm, as analysed by atomic force microscopy (AFM) (see Fig. 10) [4,117]. The same group synthesized bottlebrush block copolymers with lower-cost and more stable per(fluoro methacrylate) side-chains instead of PTF*p*HS, and these bottlebrush block copolymers exhibited preferential vertical alignment when spun cast and solvent annealed[118].
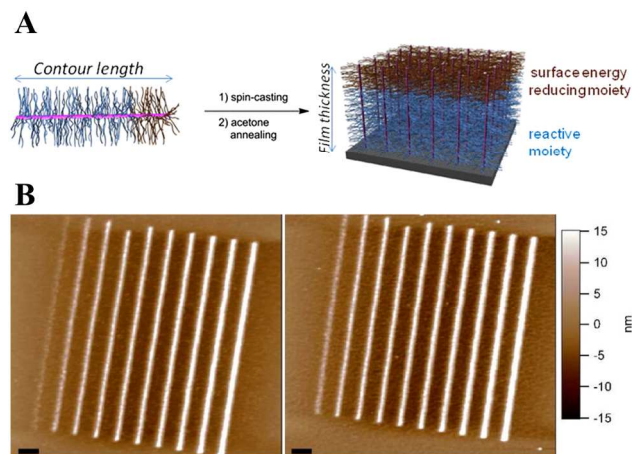
Fig. 10. Schematic and lithographic results for bottlebrush-based negative resists. A) Schematic for vertical alignment of bottlebrush block copolymers with a low surface energy block. Reprinted with permission from Trefonas et al., Copyright (2013) Society of Photo Optical Instrumentation Engineers. B) Tapping-mode AFM height images of lithographic pattern of a bottlebrush block copolymer negative resist film at exposure dosages of 250 (left) and 400 (right) $\mu C/cm^2$. Reprinted with permission from Sun et al. [4] Copyright (2013) American Chemical Society.

Non-Associating Bottlebrushes for Encapsulation and Delivery in Solution:

In this section and the one that follows, we review recent work focused on the development of bottlebrush polymers for encapsulation and delivery, signaling, and detection in solution. Bottlebrush polymers present a number of potential advantages over other polymeric assemblies for use in solution as nanoscale encapsulation and delivery agents. First, the size and shape of bottlebrush polymers is tunable through changes in the backbone and side-chain molecular weights. Second, cylindrical molecules may be advantageous for increasing retention and uptake or for targeting of specific cells or tissues[88,119]. Furthermore, the bottlebrush structure is versatile and functionalizable through reactions with the backbones, side-chains, or bottlebrush

ends. Finally, bottlebrush copolymers can assemble to form micelles, vesicles, and other novel structures in solution that are potentially useful for encapsulation and delivery. This section focuses on strategies relying on non-associating bottlebrushes in solution, primarily core-shell type bottlebrushes, and in the subsequent section we review the growing work related to bottlebrush assemblies (micelles, vesicles, etc.) in solution. In related work, a number of studies with polynorbornenes prepared *via* ROMP have shown promise for the development of multivalent ligands that can interact with cell surface proteins and be internalized by cells[120,121], but here we only discuss work with polynorbornenes with polymeric side-chains and other related bottlebrushes.

Rzayev et al. used sequential, orthogonal controlled grafting-from polymerization reactions to prepare core-shell bottlebrushes with degradable cores[19,95,122]. In the first example reported by the group, a grafting-from methodology was used to prepare bottlebrush polymers with triblock copolymer side-chains. The resulting bottlebrush polymers contained a degradable PLA core, crosslinkable PS-*co*-poly(4-(3-butenyl)styrene) (PSB) as the middle block, and a hydrolyzable PMMA outer corona block. The bottlebrushes also contained a poly(ethylene oxide methacrylate) (PEOMA) bottlebrush block as a "stopper" to prevent polymerization at the bottlebrush ends. The bottlebrushes were fully water soluble after hydrolysis of the PMMA block, and TEM analysis revealed individual, nanoscale tubes[19]. In a related publication by the same group, core-shell bottlebrushes with PLA cores, crosslinkable PSB corona, and poly(styrene-*co*-maleic anhydride) (PSMA) as a reactive outer block were prepared. The outer block could be modified with either water or amino-terminated oligo-ethylene glycol, yielding water soluble bottlebrushes. Bottlebrushes with short oligo-ethylene glycol chains in the periphery were internalized by HeLa cells, and cellular uptake was found to be reduced for

bottlebrushes with longer ethylene glycol chains or poly(acrylic acid) (PAA) chains on the periphery (see Fig. 11A). No loss of cell viability was observed when culturing cells with water-soluble bottlebrush polymers[123]. These core-shell bottlebrushes had empty cores and therefore can potentially store and transport organic hydrophobic molecules in the molecular core. In more recent work, the group demonstrated that the PSMA block could form a dual purpose block as both a crosslinkable and water-soluble corona when PSMA was modified by reaction with cysteamine[95].

Wooley et al. reported the synthesis of core-shell bottlebrush polymers with triblock copolymer side-chains. The bottlebrushes were prepared by the grafting-through ROMP of a norbornenyl PS-*b*-PMA-*b*-P*t*BA triblock copolymer. After bottlebrush synthesis, the P*t*BA block in the periphery was hydrolyzed in acid to yield a water-soluble periphery and bottlebrush polymer. The bottlebrush polymers prepared had relatively long side-chains (15.9 kg/mol) and a target backbone DP of 100. The bottlebrushes were found to be globular in DMF but form cylindrical superstructures when transferred to water by dialysis. TEM analysis revealed the formation of cylindrical assemblies by end-to-end linking of bottlebrush polymers. The cylindrical assemblies reversibly disassociated and reassembled on heating and cooling, respectively, and when transferred back to DMF[65]. Wooley at al. also synthesized hollow core bottlebrush polymers using a combination of ROMP and grafting-from nitroxide mediated polymerization. The periphery was comprised of hydrophilic and crosslinkable PAA while the core was comprised of polyisoprene. Hollow polymeric nanoparticles were prepared by crosslinking the periphery followed by degradation of the polyisoprene core[124].

Johnson and Grubbs et al. developed a series of functionalized bottlebrushes as water-soluble nanocarriers. In one example, they prepared a macromonomer with a norbornene

endgroup that was functionalized with both an oligo-ethylene glycol chain and anticancer drugs

doxorubicin (DOX) and camptothecin (CT) (see Fig. 11C). The drugs were attached through a

light-responsive molecule, and grafting-through ROMP yielded water-soluble bottlebrushes with

triggered drug release through light exposure. The cytotoxicity of all bottlebrush polymers

studied increased by more than 10 times upon UV irradiation[125]. In an alternative approach,

Johnson et al. synthesized water-soluble, UV-responsive bottlebrush drug carriers through

copper-catalyzed alkyne-azide "click to" reactions[1].

Chong et al. demonstrated the preparation of pH-responsive bottlebrush nanocarriers.

Bottlebrush polymers were prepared through the grafting-through technique with mixed PEO

and paclitaxel (PTXL) side-chains. The resulting bottlebrushes were water soluble, and exhibited

release of the anticancer drug PTXL under acidic (pH 5.5) conditions[126]. The same group also

reported amphiphilic, heterobifunctional bottlebrush polymers in which two different side-chains

were attached to each backbone repeat unit[127,128]. In one example, the authors showed that double

brush copolymers (DBCs) with PS and PEO side-chains formed Janus nanoparticles through the

intramolecular phase-separation of PEO and PS side-chains[128] (see Fig. 11B). DBCs with

hetero-grafted PEO and PLA side-chains were added to a water/toluene mixture and found to

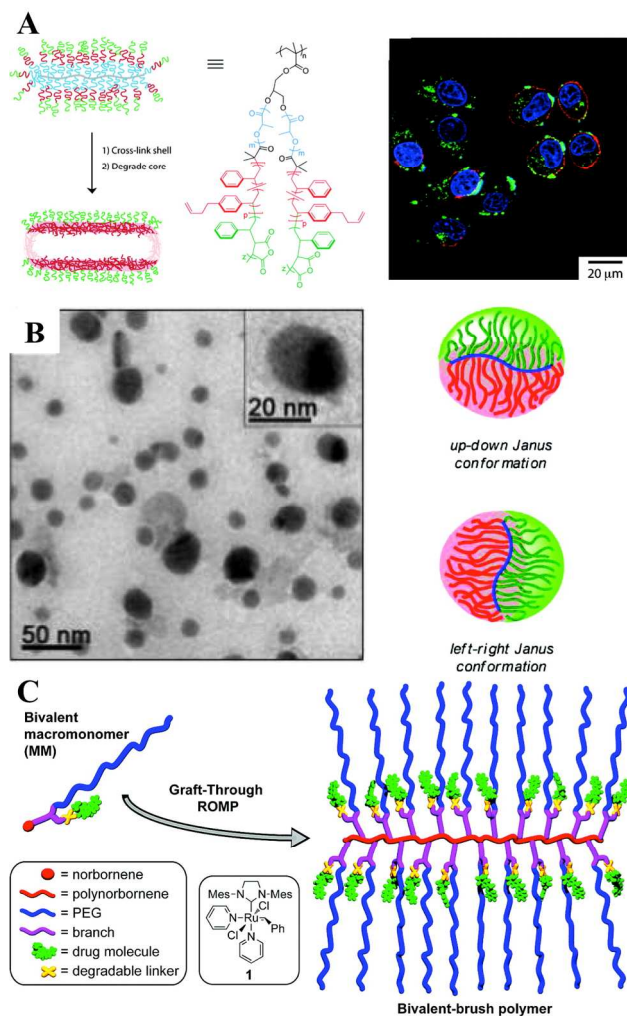stabilize mini-emulsion droplets[127].

Fig. 11. Examples of bottlebrushes for encapsulation and delivery. A) Schematic of hollow core bottlebrushes and fluorescence microscopy image showing uptake by HeLa cells. Bottlebrush polymers are tagged with fluorescein and appear green and cell nuclei appear blue. Reprinted with permission from Huan et al.[123] Copyright (2011) American Chemical Society. B) TEM analysis of bottlebrush copolymers with mixed PLA and PS side-chains and schematic for the assembly to form Janus nanoparticles. Reprinted with permission from Li et al.[128] Copyright (2012) American Chemical Society. C) Schematic for a core-shell bottlebrush with a hydrophilic periphery and a covalently bound drug molecule in the core. Reprinted with permission from Johnson et al.[125] Copyright (2010) American Chemical Society.

Zhang et al. synthesized core-shell bottlebrush polymers using a grafting-onto synthesis[129]. PLA-*b*-PEG side-chains were attached to a poly(γ-propyl-*l*-glutamate) (PPLG) backbone using copper-catalysed azide-alkyne click coupling, resulting in bottlebrushes with grafting densities of 82 – 93 %. The bottlebrushes were fully soluble in both water and THF. The bottlebrush backbone exhibited a helical conformation characteristic of the parent PPLG polymer, but the fractional helicity was found to decrease with increase side-chain length. The authors attributed this to increased steric interactions between side-chains[129].

These studies demonstrate that bottlebrush polymer size, periphery, and interior structure can be tailored for solution encapsulation and delivery. Bottlebrush polymers have a high density of chain ends and might also be useful as synthetic multivalent ligands for coupling to cell surface receptors[130].

Bottlebrush Assemblies in Solution for Delivery and Interfacial Modification:

In this section, we focus on bottlebrush systems that assemble or associate in solution. Similar to amphiphilic, linear block copolymers, amphiphilic bottlebrush block copolymers can self-assemble to form micelles in water. The resulting micelles are typically larger than those for linear diblock copolymers, and functionality can be incorporated into the bottlebrush side-chains. Applications discussed below include drug delivery and biodetection.

The Wooley group synthesized an amphiphilic bottlebrush block copolymer with PAA and PS side-chains and studied its self-assembly to form micelles. The bottlebrush block copolymer was fully soluble in DMF and formed micelles in water. Using atomic force microscopy (AFM), transmission electron microscopy (TEM), and dynamic light scattering

(DLS), the group estimated a micellar diameter of 48 nm and aggregation number of 60, smaller than that typically observed for linear block copolymer micelles[131].

Rzayev et al. prepared bottlebrush polymers with PLA and PEO methacrylate (PEOMA) side-chains and imaged aqueous micellar assemblies using cryo-TEM[10] (see Fig. 12). Depending on the molecular weight of the bottlebrush and the asymmetry in the bottlebrush structure, the bottlebrushes assembled to form spherical, cylindrical, or lamellar bilayer micelles. A model based on the analysis of small molecule surfactants could describe trends in the size and shape of micelles. Bottlebrush cores were found to be roughly 50 nm, but the overall size of the micelle (including the corona) was typically larger than 100 nm. In some cases vesicles with total lengths of several hundred nanometres were observed. This work demonstrates the self-assembly of bottlebrushes to form large (> 100 nm) nanocarriers in water[10].
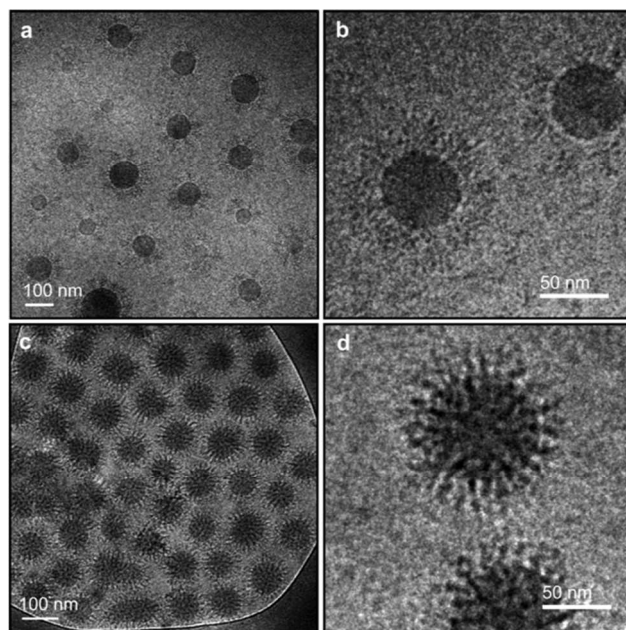

Fig. 12. Cryo-TEM images of bottlebrush copolymer assemblies in water. Reprinted with permission from Fenyves et al.[10] Copyright (2014) American Chemical Society.

Herrera et al. studied the self-assembly of amphiphilic bottlebrush copolymers with alternating PEG and PLA side-chains[50]. The bottlebrush polymers were synthesized using a combination of grafting-from and grafting-to reactions, and the final bottlebrushes had long backbone DPs (500) with short side-chains (side-chain DPs 11 – 56). The authors studied self-assembly of the amphiphilic bottlebrushes transferred to water either by multi-inlet vortex mixing, which rapidly changes the solvent environment, or by dialysis. The authors found a variety of sizes and shapes depending on the mixing conditions, and reported the formation of toroidal structures under rapid mixing and a PEG content of 26 wt %[50].

Bottlebrush assemblies can address technical challenges associated with the use of nanoparticles for high-contrast tumor imaging, as demonstrated in work by Ohe et al[41,42]. First, covalent attachment of a near-infrared fluorescence (NIRF) dye to a bottlebrush polymer prevents aggregation of the dye and self-quenching. Second, bottlebrush assemblies have a low critical micelle concentration and are more stable than linear block copolymers at dilute concentrations. Ohe et al. designed amphiphilic bottlebrush copolymers with near-infrared fluorescence (NIRF) indocyanine green (ICG) dye and targeting agents attached to the bottlebrush backbone. The amphiphilic bottlebrush block copolymers had a hydrophobic PMA side-chain block, a hydrophilic PEG side-chain block, ICG dye incorporated as side-chains for imaging, and a cyclic RDG peptides or glucosamine side-chains as targeting agents. The bottlebrush block copolymers formed micelles with diameters of roughly 200 nm and critical association concentrations in the range of $1 – 8 \ 10^{-5}$ g/L. *In vivo* studies demonstrated preferential localization of bottlebrush micelles in tumor sites[42] (Fig. 13A). In a detailed follow-up study, the authors varied the lengths of hydrophobic side-chains – using either a short alkyl side-chain or a PMA side-chain – and incorporated either hydrophilic or hydrophobic targeting

agents. Bottlebrushes with PMA side-chains as the hydrophobic block had significantly lower critical association concentrations, roughly 10^{-5} g/L compared with 10^{-3} g/L for bottlebrushes with short alkyl side-chains. Fluorescence intensity was significantly higher for bottlebrushes with the dye attached by a long side-chain compared with a short tether, and hydrophilic targeting agents were found to be more effective compared with hydrophobic targeting agents[41].
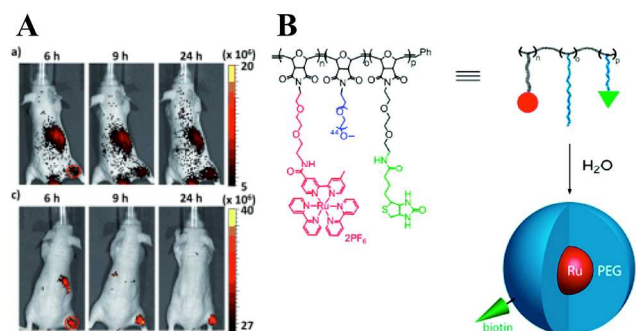

Fig. 13. Bottlebrush polymer assemblies with functionalities for tumor detection and imaging. A) NIRF images (photons per second) of tumor-bearing mice after injection of amphiphilic bottlebrush polymers with NIRF dyes. Shown are results for assemblies without (top row) and with (top row) targeting agents. Bottlebrush assemblies with targeting agents accumulate at the tumor site while bottlebrush assemblies without targeting agents accumulate at the tumor and liver. Reprinted with permission from Miki et al.[42] Copyright (2012) Wiley. B) Schematic and structure of a bottlebrush block copolymer with electrochemiluminescent metal core and biotin functionality on the periphery. Reprinted with permission from Sankaran et al.[132] Copyright (2010) American Chemical Society.

Sleiman et al. prepared biotin-functionalized, luminescent bottlebrush copolymer assemblies for biodetection assays[132,133]. The bottlebrush copolymers reported contained a hydrophilic PEG bottlebrush block, biotin functionality for binding to streptavidin, and luminescent ruthenium, iridium, or osmium polypyridine complexes (Fig 13B). These

bottlebrush block copolymers self-assembled to form spherical micelles in solution with the luminescent metals in the core and hydrophilic PEG in the corona along with biotin groups for detection. Sleiman et al. showed that placing biotin functionality on the periphery of the side-chains was necessary to get significant binding to streptavidin immobilized on beads or surfaces[133].

Johnson et al. developed a series of bottlebrush star polymers and copolymers as degradable drug carriers using a two-step synthesis approach[134–137] (Fig 14). The approach involves the preparation of living, end-functional bottlebrush arms by ROMP that are then coupled in a second reaction step with bis-norbornene crosslinker. This approach is referred to as "brush-first" since bottlebrush polymers or oligomers are first synthesized and then covalently linked to form bottlebrush star polymers and is analogous to "arm-first" synthesis approaches used to prepare star polymers by coupling linear polymer chains[138–140]. In contrast to similar "brush-first" approaches using controlled radical polymerization reactions[141], there is no residual unreacted macromonomer after the first step, and the bottlebrush star molecular weight can be controlled by varying the length of the bottlebrush arms and the molar ratio of crosslinkers. The group also incorporated a UV-responsive nitrobenzyloxycarbonyl (NBOC) crosslinker which led to bottlebrush star polymer degradation upon UV irradiation[134].
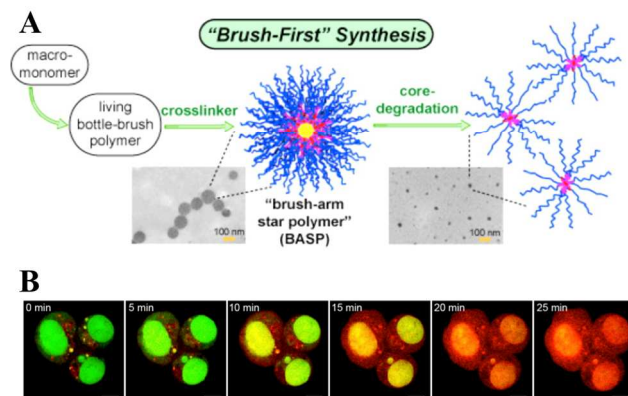
Fig. 14. "Brush-first" synthesis method for the preparation of drug-loaded star bottlebrush copolymers. A) Schematic of brush-first synthesis approach and TEM analysis of bottlebrush star polymers before and after core degradation induced by UV exposure. Reprinted with permission from Liu et al.[134] Copyright (2012) American Chemical Society. B) Live-cell confocal imaging of ovarian cancer cells exposed to DOX and cisplatin-loaded bottlebrush star polymers. The frames show cell death within 25 min. after start of UV-light exposure. Reprinted with Permission from Liao et al.[137] Copyright (2014) American Chemical Society.

Johnson et al. prepared photo-responsive drug carriers using their brush-first approach. In one example, anticancer drug doxorubicin (DOX) was covalently linked to the bottlebrush star polymers through a copper-catalyzed azide-alkyne click coupling reaction. Drug-loaded star polymers were non-toxic, and on exposure to 365 nm light DOX is released from the star polymers, as confirmed by FTIR and cell viability measurements[136]. In another study, Johnson et al. demonstrated the potential for bottlebrush star polymers to deliver multiple drugs at a desired dosage in response to distinct stimuli. Two different norbornenyl macromonomers were synthesized, containing either DOX or camptothecin (CPT). These macromonomers were mixed at a desired ratio and copolymerized with PEG macromonomer in the first step of their "brush-first" synthesis approach. The authors then coupled the brush arms using a Pt(IV) bis-norbornene complex. Hydrolysis of the bottlebrush star polymer crosslinkers thus results in release of DOX and CPT and, after reduction of the Pt(IV) complex, cytotoxic cisplatin. Confocal microscopy measurements and *in vitro* cellular viability studies were carried out to confirm internalization and cytotoxicity of drug-loaded bottlebrush star polymers[137]. In another study using the brush-first approach, Johnson et al. demonstrated the preparation of mikto-arm bottlebrush star

polymers. Analysis by TEM showed the intramolecular phase separation of the various polymer arms to form Janus nanoparticles[135].

Conclusions

Work with bottlebrush polymers has advanced tremendously over the past decade. The growing interest in bottlebrushes is due in part to the development of polymer synthesis techniques for preparing bottlebrush block copolymers and other types of bottlebrush copolymers. A variety of grafting-from and grafting-through polymer synthesis strategies are now available for reliably producing well-defined bottlebrush polymers in sufficient quantities for study in bulk, in solution, or in thin films.

Unlike linear diblock copolymers, high molecular weight bottlebrush block copolymers are unentangled and can readily self-assemble in the bulk or thin films to form large, periodic domains that are suitable for photonics[3]. The kinetics of assembly are faster for bottlebrush block copolymers compared with linear block copolymers, and an extended bottlebrush backbone also results in a higher T_{ODT}. Bottlebrushes with mixed side-chains can also self-assemble to form periodic domains of a smaller size, and the increased ordering relative to linear diblock copolymers is useful as negative tone resists for lithographic patterning[4,117].

Bottlebrush polymers can also serve as nanomaterials for targeted fluorescent imaging and drug delivery. The advantage of bottlebrush block and mixed copolymers over linear block copolymer micelles is their elongated shape, tunable size, and control over the characteristics of bottlebrush polymer molecular structure, including side-chain functionality. Bottlebrush block copolymers have a lower critical micelle concentration compared with linear diblock copolymers and surfactants. A series of bottlebrush polymers and block copolymers with different exterior

and interior structures has been demonstrated: bottlebrushes with hydrophilic exteriors and hollow interiors[95,124], bottlebrushes with covalently attached drug molecules[125,126,136], and Janus-type amphiphilic bottlebrushes[128]. Bottlebrush polymers and copolymers have been shown to provide on-demand drug release[137] with the capability for targeting through molecular recognition[133].

A number of opportunities for both fundamental and applied work with bottlebrush polymers remain, and here we address three specific areas. First, a more quantitative understanding of bottlebrush block copolymer self-assembly in the bulk and thin films is needed. For example, the role of side-chain length and backbone length on domain sizes has been studied, but how these influence T_{ODT} and domain structure (e.g. cylindrical, lamellar, etc.) has only been reported for a few systems. A more quantitative understanding leading to a predictive model of bottlebrush copolymer self-assembly would enable the design of bottlebrush copolymers to target specific self-assembled structures with desired phase behaviour.

Second, the use of bottlebrush polymers to tailor surfaces and interfaces is an emerging area. Polymer brush films[142,143], polymer-coated nanoparticles[144,145], and branched polymers[146] are effective for reducing surface fouling, enhancing film properties, or as additives for compatibilizers. Bottlebrush polymers have been shown to exhibit similar properties and spontaneously segregate to interfaces[91], but their potential for modifying films and interfaces, including liquid-liquid interfaces, is unclear. With proper design and processing, bottlebrush additives may be able to provide antifouling, self-healing, or stimuli-responsive interfacial properties similar to other brush-like polymers and polymeric nanoparticles.

Finally, solution assemblies of bottlebrush block and mixed copolymers have been explored in only a limited set of systems. A more comprehensive understanding of the phase

behaviour, kinetics, and stability of micelles and vesicles would enable the preparation of

nanomaterials with a desired size, shape, and functionality and could lead to new applications of

bottlebrush polymers for biomedical applications.

Acknowledgements

References

1   J. A. Johnson, Y. Y. Lu, A. O. Burts, Y.-H. Lim, M. G. Finn, J. T. Koberstein, N. J. Turro, D. A. Tirrell and R. H. Grubbs, *J. Am. Chem. Soc.*, 2010, **133**, 559–566.
2   X. Li, S. L. Prukop, S. L. Biswal and R. Verduzco, *Macromolecules*, 2012, **45**, 7118–7127.
3   G. M. Miyake, V. A. Piunova, R. A. Weitekamp and R. H. Grubbs, *Angew. Chem. Int. Ed.*, 2012, **51**, 11246–11248.
4   G. Sun, S. Cho, C. Clark, S. V. Verkhoturov, M. J. Eller, A. Li, A. Pavía-Jiménez, E. A. Schweikert, J. W. Thackeray, P. Trefonas and K. L. Wooley, *J. Am. Chem. Soc.*, 2013, **135**, 4203–4206.
5   P. Masson, E. Franta and P. Rempp, *Makromol. Chem. Rapid Commun.*, 1982, **3**, 499–504.
6   P. Rempp, P. Lutz, P. Masson and P. Chaumont, *Makromol. Chem.*, 1985, **13**, 47–66.
7   S. L. Pesek, X. Li, B. Hammouda, K. Hong and R. Verduzco, *Macromolecules*, 2013, **46**, 6998–7005.
8   A. Nese, Y. Kwak, R. Nicolaÿ, M. Barrett, S. S. Sheiko and K. Matyjaszewski, *Macromolecules*, 2010, **43**, 4016–4019.
9   H.-P. Hsu, K. Binder and W. Paul, *Phys. Rev. Lett.*, 2009, **103**, 198301.
10   R. Fenyves, M. Schmutz, I. J. Horner, F. V. Bright and J. Rzayev, *J. Am. Chem. Soc.*, 2014, **136**, 7762–7770.
11   J. Rzayev, *ACS Macro Lett.*, 2012, **1**, 1146–1149.
12   S. S. Sheiko, B. S. Sumerlin and K. Matyjaszewski, *Prog. Polym. Sci.*, 2008, **33**, 759–785.

13   J. Yuan, A. H. E. Müller, K. Matyjaszewski and S. S. Sheiko, in *Polymer Science: A Comprehensive Reference*, eds. K. Matyjaszewski and M. Möller, Elsevier, Amsterdam, 2012, pp. 199–264.

14   H. Lee, J. Pietrasik, S. S. Sheiko and K. Matyjaszewski, *Prog. Polym. Sci.*, 2010, **35**, 24–44.

15   C. Feng, Y. Li, D. Yang, J. Hu, X. Zhang and X. Huang, *Chem. Soc. Rev.*, 2011, **40**, 1282–1295.

16   Y. Chen, *Macromolecules*, 2012, **45**, 2619–2631.

17   K. L. Beers, S. G. Gaynor, K. Matyjaszewski, S. S. Sheiko and M. Moller, *Macromolecules*, 1998, **31**, 9413–9415.

18   H. G. Börner, D. Duran, K. Matyjaszewski, M. da Silva and S. S. Sheiko, *Macromolecules*, 2002, **35**, 3387–3394.

19   K. Huang and J. Rzayev, *J. Am. Chem. Soc.*, 2009, **131**, 6880–6885.

20   J. Bolton and J. Rzayev, *Macromolecules*, 2014, **47**, 2864–2874.

21   J. Bolton and J. Rzayev, *ACS Macro Lett.*, 2012, **1**, 15–18.

22   Y. Xia, J. A. Kornfield and R. H. Grubbs, *Macromolecules*, 2009, **42**, 3761–3766.

23   H. Gao and K. Matyjaszewski, *J. Am. Chem. Soc.*, 2007, **129**, 6633–6639.

24   Y. Tsukahara, K. Mizuno, A. Segawa and Y. Yamashita, *Macromolecules*, 1989, **22**, 1546–1552.

25   Y. Tsukahara, K. Tsutsumi, Y. Yamashita and S. Shimada, *Macromolecules*, 1989, **22**, 2869–2871.

26   Y. Tsukahara, K. Tsutsumi, Y. Yamashita and S. Shimada, *Macromolecules*, 1990, **23**, 5201–5208.

27   Y. Tsukahara, S. Kohjiya, K. Tsutsumi and Y. Okamoto, *Macromolecules*, 1994, **27**, 1662–1664.

28   M. Wintermantel, K. Fischer, M. Gerle, R. Ries, M. Schmidt, K. Kajiwara, H. Urakawa and I. Wataoka, *Angew Chem Int Ed*, 1995, **34**, 1472–1474.

29   M. Wintermantel, M. Gerle, K. Fischer, M. Schmidt, I. Wataoka, H. Urakawa, K. Kajiwara and Y. Tsukahara, *Macromolecules*, 1996, **29**, 978–983.

30   I. Wataoka, H. Urakawa, K. Kajiwara, M. Schmidt and M. Wintermantel, *Polym. Int.*, 1997, **44**, 365–370.

31   P. Dziezok, K. Fischer, M. Schmidt, S. S. Sheiko and M. Möller, *Angew Chem Int Ed*, 1997, **36**, 2812–2815.

32   S. Jha, S. Dutta and N. B. Bowden, *Macromolecules*, 2004, **37**, 4365–4374.

33   Y. Xia, B. D. Olsen, J. A. Kornfield and R. H. Grubbs, *J. Am. Chem. Soc.*, 2009, **131**, 18525–18532.

34   C. Hou, J. Hu, G. Liu, J. Wang, F. Liu, H. Hu, G. Zhang, H. Zou, Y. Tu and B. Liao, *Macromolecules*, 2013, **46**, 4053–4063.

35   M. Schappacher and A. Deffieux, *Macromolecules*, 2005, **38**, 7209–7213.

36   D. Lanson, F. Ariura, M. Schappacher, R. Borsali and A. Deffieux, *Macromolecules*, 2009, **42**, 3942–3950.

37   P. Chen, C. Li, D. Liu and Z. Li, *Macromolecules*, 2012, **45**, 9579–9584.

38   A. C. Engler, H. Lee and P. T. Hammond, *Angew. Chem. Int. Ed.*, 2009, **48**, 9334–9338.

39   I. Gadwal, J. Rao, J. Baettig and A. Khan, *Macromolecules*, 2014, **47**, 35–40.

40   S. De and A. Khan, *Chem. Commun.*, 2012, **48**, 3130–3132.

41   K. Miki, K. Oride, A. Kimura, Y. Kuramochi, H. Matsuoka, H. Harada, M. Hiraoka and K. Ohe, *Small*, 2011, **7**, 3536–3547.

42   K. Miki, A. Kimura, K. Oride, Y. Kuramochi, H. Matsuoka, H. Harada, M. Hiraoka and K. Ohe, *Angew. Chem. Int. Ed.*, 2011, **50**, 6567–6570.

43   US8283428 B2, .

44　D. F. Zeigler, K. A. Mazzio and C. K. Luscombe, *Macromolecules*, 2014.

45　S. Zhou, Y. Zhou, H. Tian, Y. Zhu, Y. Pan, F. Zhou, Q. Zhang, Z. Shen and X. Fan, *J. Polym. Sci. Part Polym. Chem.*, 2014, **52**, 1519–1524.

46　R. Sugi, D. Tate and T. Yokozawa, *J. Polym. Sci. Part Polym. Chem.*, 2013, **51**, 2725–2729.

47　E.-H. Kang, I.-H. Lee and T.-L. Choi, *ACS Macro Lett.*, 2012, **1**, 1098–1102.

48　M. J. Allen, K. Wangkanont, R. T. Raines and L. L. Kiessling, *Macromolecules*, 2009, **42**, 4023–4027.

49　A. M. Anderson-Wile, G. W. Coates, F. Auriemma, C. De Rosa and A. Silvestre, *Macromolecules*, 2012, **45**, 7863–7877.

50　H. Luo, J. L. Santos and M. Herrera-Alonso, *Chem. Commun.*, 2013, **50**, 536–538.

51　D. Zehm, A. Laschewsky, H. Liang and J. P. Rabe, *Macromolecules*, 2011, **44**, 9635–9641.

52　A. Li, Z. Li, S. Zhang, G. Sun, D. M. Policarpio and K. L. Wooley, *ACS Macro Lett.*, 2012, **1**, 241–245.

53　A. O. Moughton, T. Sagawa, W. M. Gramlich, M. Seo, T. P. Lodge and M. A. Hillmyer, *Polym. Chem.*, 2012, **4**, 166–173.

54　Q. Fu, J. M. Ren and G. G. Qiao, *Polym. Chem.*, 2012, **3**, 343–351.

55　Y. Shi, W. Zhu and Y. Chen, *Macromolecules*, 2013, **46**, 2391–2398.

56　E. Kutnyánszky, M. A. Hempenius and G. J. Vancso, *Polym. Chem.*, 2013, **5**, 771–783.

57　S. S. Sheiko, F. C. Sun, A. Randall, D. Shirvanyants, M. Rubinstein, H. Lee and K. Matyjaszewski, *Nature*, 2006, **440**, 191–194.

58　J. Pietrasik, B. S. Sumerlin, R. Y. Lee and K. Matyjaszewski, *Macromol. Chem. Phys.*, 2007, **208**, 30–36.

59　J. Bolton, T. S. Bailey and J. Rzayev, *Nano Lett.*, 2011, **11**, 998–1001.

60　I. Park, A. Nese, J. Pietrasik, K. Matyjaszewski and S. S. Sheiko, *J. Mater. Chem.*, 2011, **21**, 8448–8453.

61　C. Cheng, E. Khoshdel and K. L. Wooley, *Nano Lett.*, 2006, **6**, 1741–1746.

62　J. Rzayev, *Macromolecules*, 2009, **42**, 2135–2141.

63　D. Le, V. Montembault, J. C. Soutif, M. Rutnakornpituk and L. Fontaine, *Macromolecules*, 2010, **43**, 5611–5617.

64　Z. Li, K. Zhang, J. Ma, C. Cheng and K. L. Wooley, *J. Polym. Sci. Part Polym. Chem.*, 2009, **47**, 5557–5563.

65　Z. Li, J. Ma, N. S. Lee and K. L. Wooley, *J. Am. Chem. Soc.*, 2011, **133**, 1228–1231.

66　S. Ahn, D. L. Pickel, W. M. Kochemba, J. Chen, D. Uhrig, J. P. Hinestrosa, J.-M. Carrillo, M. Shao, C. Do, J. M. Messman, W. M. Brown, B. G. Sumpter and S. M. Kilbey, *ACS Macro Lett.*, 2013, 761–765.

67　T. Li, J. Lin, T. Chen and S. Zhang, *Polymer*, 2006, **47**, 4485–4489.

68　L. Feuz, P. Strunz, T. Geue, M. Textor and O. Borisov, *Eur. Phys. J. E*, 2007, **23**, 237–245.

69　S. S. Sheiko, S. A. Prokhorova, K. L. Beers, K. Matyjaszewski, I. I. Potemkin, A. R. Khokhlov and M. Möller, *Macromolecules*, 2001, **34**, 8354–8360.

70　S. S. Sheiko and M. Möller, *Chem. Rev. Wash. DC U. S.*, 2001, **101**, 4099–4124.

71　M. Gerle, K. Fischer, S. Roos, A. H. E. Muller, M. Schmidt, S. S. Sheiko, S. Prokhorova and M. Moller, *Macromolecules*, 1999, **32**, 2629–2637.

72　P. J. M. Stals, Y. Li, J. Burdyńska, R. Nicolaÿ, A. Nese, A. R. A. Palmans, E. W. Meijer, K. Matyjaszewski and S. S. Sheiko, *J. Am. Chem. Soc.*, 2013, **135**, 11421–11424.

73　S. S. Sheiko, J. Zhou, J. Arnold, D. Neugebauer, K. Matyjaszewski, C. Tsitsilianis, V. V. Tsukruk, J.-M. Y. Carrillo, A. V. Dobrynin and M. Rubinstein, *Nat. Mater.*, 2013, **12**, 735–740.

74 F. C. Sun, A. V. Dobrynin, D. Shirvanyants, H.-I. Lee, K. Matyjaszewski, G. J. Rubinstein, M. Rubinstein and S. S. Sheiko, *Phys. Rev. Lett.*, 2007, **99**, 137801.

75 S. Rathgeber, H. Lee, K. Matyjaszewski and E. Di Cola, *Macromolecules*, 2007, **40**, 7680–7688.

76 S. Rathgeber, T. Pakula, A. Wilk, K. Matyjaszewski, H. Lee and K. L. Beers, *Polymer*, 2006, **47**, 7318–7327.

77 S. Rathgeber, T. Pakula, A. Wilk, K. Matyjaszewski and K. L. Beers, *J. Chem. Phys.*, 2005, **122**, 124904–13.

78 S. J. Dalsin, M. A. Hillmyer and F. S. Bates, *ACS Macro Lett.*, 2014, **3**, 423–427.

79 I. I. Potemkin, A. R. Khokhlov and P. Reineker, *Eur. Phys. J. E*, 2001, **4**, 93–101.

80 T. M. Birshtein, O. V. Borisov, Y. B. Zhulina, A. R. Khokhlov and T. A. Yurasova, *Polym. Sci. USSR*, 1987, **29**, 1293–1300.

81 G. H. Fredrickson, *Macromolecules*, 1993, **26**, 2825–2831.

82 H.-P. Hsu, W. Paul and K. Binder, *Macromol. Theory Simul.*, 2007, **16**, 660–689.

83 N. A. Denesyuk, *Phys. Rev. E*, 2003, **67**, 051803.

84 S. Panyukov, E. B. Zhulina, S. S. Sheiko, G. C. Randall, J. Brock and M. Rubinstein, *J. Phys. Chem. B*, 2009, **113**, 3750–3768.

85 H.-P. Hsu, W. Paul and K. Binder, *J. Chem. Phys.*, 2008, **129**, 204904–11.

86 H.-P. Hsu, W. Paul and K. Binder, *Macromol. Theory Simul.*, 2011, **20**, 510–525.

87 M. Hu, Y. Xia, G. B. McKenna, J. A. Kornfield and R. H. Grubbs, *Macromolecules*, 2011, **44**, 6935–6943.

88 Y. Geng, P. Dalhaimer, S. Cai, R. Tsai, M. Tewari, T. Minko and D. E. Discher, *Nat Nano*, 2007, **2**, 249–255.

89 S. S. Sheiko, S. Panyukov and M. Rubinstein, *Macromolecules*, 2011, **44**, 4520–4529.

90 M. J. Barrett, F. C. Sun, A. Nese, K. Matyjaszewski, J.-M. Y. Carrillo, A. V. Dobrynin and S. S. Sheiko, *Langmuir*, 2010, **26**, 15339–15344.

91 I. Mitra, X. Li, S. L. Pesek, B. Makarenko, B. S. Lokitz, D. Uhrig, J. F. Ankner, R. Verduzco and G. E. Stein, *Macromolecules*, 2014, **47**, 5269–5276.

92 Y. Xia, Y. Li, A. O. Burts, M. F. Ottaviani, D. A. Tirrell, J. A. Johnson, N. J. Turro and R. H. Grubbs, *J. Am. Chem. Soc.*, 2011, **133**, 19953–19959.

93 Z. Zhang, J.-M. Y. Carrillo, S. Ahn, B. Wu, K. Hong, G. S. Smith and C. Do, *Macromolecules*, 2014, **47**, 5808–5814.

94 D. Uhrig and J. Mays, *Polym. Chem.*, 2011, **2**, 69–76.

95 K. Huang, M. Johnson and J. Rzayev, *ACS Macro Lett.*, 2012, **1**, 892–895.

96 M. B. Runge, J. Yoo and N. B. Bowden, *Macromol. Rapid Commun.*, 2009, **30**, 1392–1398.

97 M. B. Runge, S. Dutta and N. B. Bowden, *Macromolecules*, 2006, **39**, 498–508.

98 M. B. Runge and N. B. Bowden, *J. Am. Chem. Soc.*, 2007, **129**, 10551–10560.

99 M. B. Runge, C. E. Lipscomb, L. R. Ditzler, M. K. Mahanthappa, A. V. Tivanski and N. B. Bowden, *Macromolecules*, 2008, **41**, 7687–7694.

100 J. Yoo, M. B. Runge and N. B. Bowden, *Polymer*, 2011, **52**, 2499–2504.

101 G. H. Fredrickson and F. S. Bates, *Annu. Rev. Mater. Sci.*, 1996, **26**, 501–550.

102 I. W. Hamley, *The Physics of Block Copolymers*, Oxford University Press, Oxford, 1998.

103 S. W. Hong, W. Gu, J. Huh, B. R. Sveinbjornsson, G. Jeong, R. H. Grubbs and T. P. Russell, *ACS Nano*, 2013, **7**, 9684–9692.

104 W. Gu, J. Huh, S. W. Hong, B. R. Sveinbjornsson, C. Park, R. H. Grubbs and T. P. Russell, *ACS Nano*, 2013, **7**, 2551–2558.

105 M. Byun, W. Han, F. Qiu, N. B. Bowden and Z. Lin, *Small*, 2010, **6**, 2250–2255.

106 M. Byun, N. B. Bowden and Z. Lin, *Nano Lett.*, 2010, **10**, 3111–3117.

107 P. Deshmukh, S. Ahn, L. Geelhand de Merxem and R. M. Kasi, *Macromolecules*, 2013, **46**, 8245–8252.

108 P. Deshmukh, S. Ahn, M. Gopinadhan, C. O. Osuji and R. M. Kasi, *Macromolecules*, 2013, **46**, 4558–4566.

109 P. Deshmukh, M. Gopinadhan, Y. Choo, S. Ahn, P. W. Majewski, S. Y. Yoon, O. Bakajin, M. Elimelech, C. O. Osuji and R. M. Kasi, *ACS Macro Lett.*, 2014, **3**, 462–466.

110 John D. Joannopoulos, Steven G. Johnson, Joshua N. Winn and Robert D. Meade, *Photonic Crystals: Molding the Flow of Light*, Princeton University Press, Princeton, 2nd edn., 1995.

111 J. Yoon, W. Lee and E. L. Thomas, *MRS Bull.*, 2005, **30**, 721–726.

112 B. R. Sveinbjörnsson, R. A. Weitekamp, G. M. Miyake, Y. Xia, H. A. Atwater and R. H. Grubbs, *Proc. Natl. Acad. Sci.*, 2012, **109**, 14332–14336.

113 Y. Kang, J. J. Walish, T. Gorishnyy and E. L. Thomas, *Nat. Mater.*, 2007, **6**, 957–960.

114 G. M. Miyake, R. A. Weitekamp, V. A. Piunova and R. H. Grubbs, *J. Am. Chem. Soc.*, 2012, **134**, 14249–14254.

115 V. A. Piunova, G. M. Miyake, C. S. Daeffler, R. A. Weitekamp and R. H. Grubbs, *J. Am. Chem. Soc.*, 2013, **135**, 15609–15616.

116 I. Luzinov, S. Minko and V. V. Tsukruk, *Prog. Polym. Sci.*, 2004, **29**, 635–698.

117 P. Trefonas, J. W. Thackeray, G. Sun, S. Cho, C. Clark, S. V. Verkhoturov, M. J. Eller, A. Li, A. Pavia-Sanders, E. A. Schweikert and K. L. Wooley, *J. MicroNanolithography MEMS MOEMS*, 2013, **12**, 043006–043006.

118 S. Cho, F. Yang, G. Sun, M. J. Eller, C. Clark, E. A. Schweikert, J. W. Thackeray, P. Trefonas and K. L. Wooley, *Macromol. Rapid Commun.*, 2014, **35**, 437–441.

119 S. Venkataraman, J. L. Hedrick, Z. Y. Ong, C. Yang, P. L. R. Ee, P. T. Hammond and Y. Y. Yang, *Adv. Drug Deliv. Rev.*, 2011, **63**, 1228–1246.

120 E. M. Kolonko, J. K. Pontrello, S. L. Mangold and L. L. Kiessling, *J. Am. Chem. Soc.*, 2009, **131**, 7327–7333.

121 K. Lienkamp, A. E. Madkour, A. Musante, C. F. Nelson, Klaus Nüsslein and G. N. Tew, *J. Am. Chem. Soc.*, 2008, **130**, 9836–9843.

122 K. Huang, D. P. Canterbury and J. Rzayev, *Macromolecules*, 2010, **43**, 6632–6638.

123 K. Huang, A. Jacobs and J. Rzayev, *Biomacromolecules*, 2011, **12**, 2327–2334.

124 C. Cheng, K. Qi, E. Khoshdel and K. L. Wooley, *J. Am. Chem. Soc.*, 2006, **128**, 6808–6809.

125 J. A. Johnson, Y. Y. Lu, A. O. Burts, Y. Xia, A. C. Durrell, D. A. Tirrell and R. H. Grubbs, *Macromolecules*, 2010, **43**, 10326–10335.

126 J. Zou, G. Jafr, E. Themistou, Y. Yap, Z. A. P. Wintrob, P. Alexandridis, A. C. Ceacareanu and C. Cheng, *Chem. Commun.*, 2011, **47**, 4493–4495.

127 Y. Li, J. Zou, B. P. Das, M. Tsianou and C. Cheng, *Macromolecules*, 2012, **45**, 4623–4629.

128 Y. Li, E. Themistou, J. Zou, B. P. Das, M. Tsianou and C. Cheng, *ACS Macro Lett.*, 2012, **1**, 52–56.

129 H. Tang, Y. Li, S. H. Lahasky, S. S. Sheiko and D. Zhang, *Macromolecules*, 2011, **44**, 1491–1499.

130 L. L. Kiessling, J. E. Gestwicki and L. E. Strong, *Angew. Chem. Int. Ed.*, 2006, **45**, 2348–2368.

131 Z. Li, J. Ma, C. Cheng, K. Zhang and K. L. Wooley, *Macromolecules*, 2010, **43**, 1182–1184.

132 N. B. Sankaran, A. Z. Rys, R. Nassif, M. K. Nayak, K. Metera, B. Chen, H. S. Bazzi and H. F. Sleiman, *Macromolecules*, 2010, **43**, 5530–5537.

133 K. L. Metera, K. D. Hänni, G. Zhou, M. K. Nayak, H. S. Bazzi, D. Juncker and H. F. Sleiman, *ACS Macro Lett.*, 2012, **1**, 954–959.

134 J. Liu, A. O. Burts, Y. Li, A. V. Zhukhovitskiy, M. F. Ottaviani, N. J. Turro and J. A. Johnson, *J. Am. Chem. Soc.*, 2012, **134**, 16337–16344.

135 A. O. Burts, A. X. Gao and J. A. Johnson, *Macromol. Rapid Commun.*, 2014, **35**, 168–173.

136 A. O. Burts, L. Liao, Y. Y. Lu, D. A. Tirrell and J. A. Johnson, *Photochem. Photobiol.*, 2014, **90**, 380–385.

137 L. Liao, J. Liu, E. C. Dreaden, S. W. Morton, K. E. Shopsowitz, P. T. Hammond and J. A. Johnson, *J. Am. Chem. Soc.*, 2014, **136**, 5896–5899.

138 R. S. Saunders, R. E. Cohen, S. J. Wong and R. R. Schrock, *Macromolecules*, 1992, **25**, 2055–2057.

139 A. Kohler, J. G. Zilliox, P. Rempp, J. Polacek and I. Koessler, *Eur. Polym. J.*, 1972, **8**, 627–639.

140 J. Xia, X. Zhang and K. Matyjaszewski, *Macromolecules*, 1999, **32**, 4482–4484.

141 H. Gao, S. Ohno and K. Matyjaszewski, *J. Am. Chem. Soc.*, 2006, **128**, 15111–15113.

142 W. J. Yang, K.-G. Neoh, E.-T. Kang, S. L.-M. Teo and D. Rittschof, *Prog. Polym. Sci.*, 2014, **39**, 1017–1042.

143 A. Hucknall, S. Rangarajan and A. Chilkoti, *Adv. Mater.*, 2009, **21**, 2441–2446.

144 S. K. Kumar, N. Jouault, B. Benicewicz and T. Neely, *Macromolecules*, 2013, **46**, 3199–3214.

145 J. Kim and P. F. Green, *Macromolecules*, 2010, **43**, 1524–1529.

146 J. W. Bartels, C. Cheng, K. T. Powell, J. Xu and K. L. Wooley, *Macromol. Chem. Phys.*, 2007, **208**, 1676–1687.